

Molecular Engineering. 8.¹ Kinetic and Conformational Studies of Resorcin[4]arene-Based C₄ Tetraoxatetraethiahemicarceplexes: Carceroisomerism and Twistomerism

Kyungsoo Paek,^{*,†} Hyejae Ihm,[†] Sunggoo Yun,[‡] Hee Cheon Lee,[‡] and Kyoung Tai No[†]

Molecular Engineering Research Laboratory and Department of Chemistry, Soongsil University, Seoul 156-743, Korea, and Department of Chemistry, Pohang University of Science & Technology, Pohang 790-784, Korea

kpaek@saint.ssu.ac.kr

Received February 27, 2001

New C_{4v} tetraoxatetraethiahemicarcerands and their six hemicarceplexes containing DMF, DMA, DMSO, or NMP were synthesized and characterized. Their conformations, kinetic properties, carceroisomerism, and twistomerism were studied by VT, 2D COSY, NOESY, and ROESY ¹H NMR experiments. The decomplexation rates of DMF or DMA were very slow with high activation energy barriers (73 and 104 kJ mol⁻¹, respectively) and the complexed guests feel more constriction than their free liquid state. The largest isomerization energy barrier of carceroisomers was 15.4 kcal mol⁻¹, and the isomerization energy barriers of twistomers are significantly larger than those of carceroisomers.

Introduction

The potential applicabilities of container molecules² are being expanded from a molecular recognition system³ or a supramolecular molecular storage⁴ to a controlled molecular releasing system⁵ or molecular reactor.⁶ Also, new types of isomerisms in a confined carceplex or a hemicarceplex are emerging as a stimulating research field due to their potential as a molecular spin or molecular switch for data storage device and molecular electronics.⁷ D_{4h} and C_{4v} container hosts composed of two resorcin[4]arene moieties could lead pseudohelical ste-

reoisomers, so-called twistomers,^{7d} stabilized by the host's constrictive binding property. In C_{4v} carcerand composed of two different hemispheres, the different orientations of unsymmetrical guests through the long (C₄) axis of these host could also lead different stereoisomers, which Reinhoudt et al. called carceroisomer.^{7a}

Usually carceroisomer interconversion, which appears to be faster than twistomer interconversion,^{7d} could be manipulated by the degree of confinement of interior and the secondary interactions between host and guest such as hydrogen bonding, dipole, or charge interactions, whereas twistomer interconversion could be manipulated by constrictive binding property of host. The constrictive binding property mainly depends on the nature of bridges, such as the number and length, connecting two hemispheres as well as the nature of hemisphere.² But the effects of molecular symmetry or heavy atoms on bridge have not been scrutinized.⁸ Here we report the kinetic and conformational properties of new resorcin[4]-arene-based C₄ tetraoxatetraethiahemicarcerands, which have sulfur-incorporated unsymmetric bridges between two hemispheres. High-temperature stable carceroisomers and the unprecedented half-twistomers were characterized.

Results and Discussion

Synthesis of Hemicarcerand and Hemicarceplexes. Tetrathiol **2** was obtained from tetrabromide **1** (92%),⁹ and tetrols **3**¹⁰ and **4**¹¹ were obtained from the corre-

* To whom correspondence should be addressed. Tel: (+) 82-2-820-0435. Fax: (+) 82-2-822-2362.

[†] Soongsil University.

[‡] Pohang University of Science and Technology.

(1) Paek, K.; Yoon, Y.; Suh, Y. *J. Chem. Soc., Perkin Trans. 2* **2001**, (6), 916.

(2) (a) Cram, D. J.; Cram, J. M. *Container Molecules and Their Guests, Monographs in Supramolecular Chemistry*; Stoddart, J. F., Ed.; The Royal Society of Chemistry Press: Cambridge, 1994; Vol. 4. (b) Maverick, E. F.; Cram, D. J. In *Comprehensive Supramolecular Chemistry*; Atwood, H. L.; Davies, J. E. D., MacNicol, D. D., Voegtle, F., Eds.; Pergamon: Oxford, U.K., 1996; Vol. 2, Chapter 12.

(3) (a) Judice, J. K.; Cram, D. J. *J. Am. Chem. Soc.* **1991**, *113*, 2790. (b) Schally, C. A.; Martin, T.; Obst, U.; Rebek, J., Jr. *J. Am. Chem. Soc.* **1999**, *121*, 2133. (c) Heinz, T.; Rudkevich, D. M.; Rebek, J., Jr. *Angew. Chem., Int. Ed. Engl.* **1999**, *38*, 1136. (d) Rivera, J. M.; Craig, S. L.; Martin, T.; Rebek, J., Jr. *Angew. Chem., Int. Ed. Engl.* **2000**, *39*, 2130.

(4) (a) Murayama, K.; Aoki, K. *Chem. Commun.* **1998**, 607. (b) Chopra, N.; Sherman, J. C. *Angew. Chem., Int. Ed.* **1999**, *38*, 1955. (c) Chopra, N.; Naumann, C.; Sherman, J. C. *Angew. Chem., Int. Ed.* **2000**, *39*, 194. (d) Parac, T. N.; Scherer, M.; Raymond, K. N. *Angew. Chem., Int. Ed.* **2000**, *39*, 1239. (e) Yu, S.-Y.; Kusakawa, T.; Biradha, K.; Fujita, M. *J. Am. Chem. Soc.* **2000**, *122*, 2665. (f) Yoshizawa, M.; Kusakawa, T.; Fujita, M.; Yamaguchi, K. *J. Am. Chem. Soc.* **2000**, *122*, 6311.

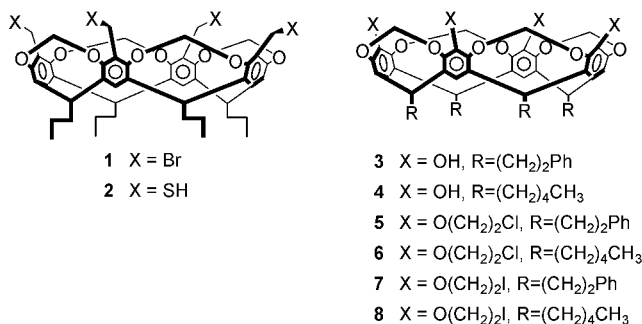
(5) (a) Cram, D. J.; Blanda, M. T.; Paek, K.; Knobler, C. B. *J. Am. Chem. Soc.* **1992**, *114*, 7765. (b) Piatnitski, E. L.; Deshayes, K. D. *Angew. Chem., Int. Ed.* **1998**, *37*, 970. (c) Vysotsky, M. O.; Thondorf, I.; Boehmer, V. *Angew. Chem., Int. Ed.* **2000**, *39*, 1264.

(6) (a) Cram, D. J.; Tanner, M. E.; Thomas, R. *Angew. Chem., Int. Ed. Engl.* **1991**, *30*, 1024. (b) Robbins, T. A.; Knobler, C. B.; Bellew, D. R.; Cram, D. J. *J. Am. Chem. Soc.* **1994**, *116*, 111. (c) Kang, J.; Santamaria, J.; Hilmerssohn, G.; Rebek, J., Jr. *J. Am. Chem. Soc.* **1998**, *120*, 7389. (d) Warmuth, R.; Marvel, M. A. *Angew. Chem., Int. Ed.* **2000**, *39*, 1117. (e) Warmuth, R. *J. Inclusion Phenom.* **2000**, *37*, 1. (f) Warmuth, R. *Eur. J. Org. Chem.* **2001**, 423.

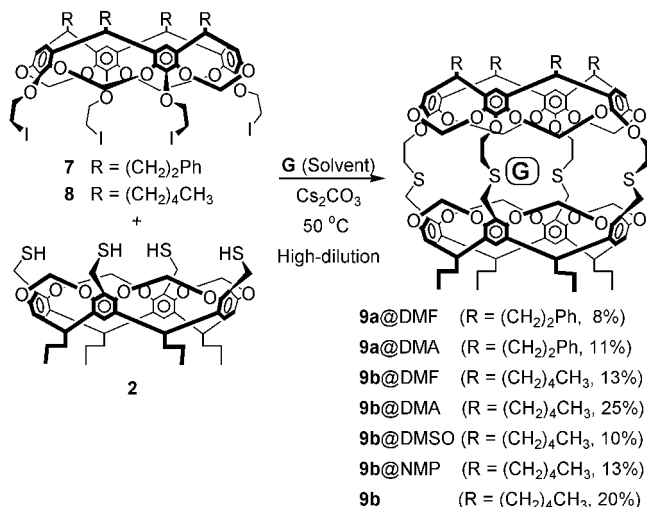
(7) (a) Timmerman, P.; Verboom, W.; van Veggel, F. C. J. M.; van Duynhoven, J. P. M.; Reinhoudt, D. N. *Angew. Chem., Int. Ed. Engl.* **1994**, *33*, 2345. (b) Huisman, B.-H.; Rudkevich, D. M.; van Veggel, F. C. J. M.; Reinhoudt, D. N. *J. Am. Chem. Soc.* **1996**, *118*, 3523. (c) van Wageningen, A. M. A.; Timmermann, P.; van Duynhoven, J. P. M.; Verboom, W.; van Veggel, F. C. J. M.; Reinhoudt, D. N. *Chem. Eur. J.* **1997**, *3*, 639. (d) Chapman, R. G.; Sherman, J. C. *J. Am. Chem. Soc.* **1999**, *121*, 1962.

(8) Paek, K.; Ihm, H.; Yun, S.; Lee, H. C. *Tetrahedron Lett.* **1999**, *40*, 8905.

Chart 1



Scheme 1



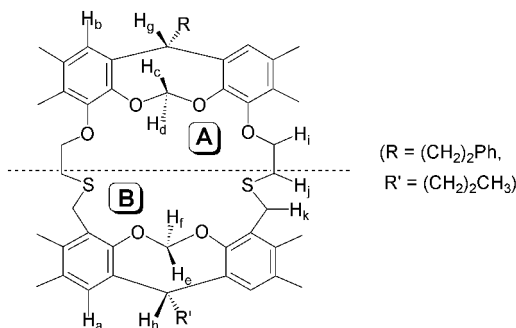
sponding tetrabromides (Chart 1). Tetrols **3** and **4** were treated with TsO(CH₂)₂Cl/K₂CO₃/DMF at 55 °C to give the tetrachlorides **5** (69%) and **6** (65%), respectively. Tetrachlorides **5** and **6** were refluxed with NaI in methyl ethyl ketone to give the tetraiodides **7** (87%) and **8** (90%), respectively.

Both tetraiodides **7** and **8** were used to synthesize the hemicarceplexes because it has been shown that PhCH₂CH₂-appended hemicarceplexes tend to produce better crystals for structure determination, whereas those with CH₃(CH₂)₄-appended groups tend to be soluble in a greater range of solvents.¹¹

Under high dilution conditions, the shell-closing reaction between tetrathiol **2** and tetraiodide **7** or **8** with Cs₂CO₃ in an appropriate solvent (G) at 50 °C produced hemicarceplexes **9a@G** or **9b@G** in 8–25% yields (Scheme 1). All hemicarceplexes were characterized by ¹H NMR, FAB+ mass, and IR spectra and elemental analyses, and the spacial arrangements between host and guest were studied by 2D COSY, NOESY, and ROESY measurements (500 MHz, CD₂Cl₂, 25 °C).

CPK molecular model studies suggest that hosts **9a** and **9b** are hemicarceplexes having the cavity large enough to include 1-methyl-2-piperidone or 1,4-dimethoxybenzene. To obtain the various hemicarceplexes, *N,N*-dimethylformamide (DMF), *N,N*-dimethylacetamide

Chart 2



(DMA), dimethyl sulfoxide (DMSO), *N*-methyl-2-pyrrolidinone (NMP), pyrazine, and 1,4-dioxane were used as solvents. Although large templating effects of pyrazine and 1,4-dioxane for resorcin[4]arene-based carcerands were reported,¹² host **9a** or **9b** complexed with pyrazine or 1,4-dioxane was not detected. It is presumable that due to the large sulfur or iodide atoms a potential template should be oriented through the long C₄ axis. In the case of pyrazine or 1,4-dioxane, its lone pair should be directed toward π-cloud of hemispheres, which subsequently diminishes their templating ability, whereas when acetonitrile was employed as a solvent, the free hemicarceplex **9b** was isolated in 20% yield. The FAB mass spectra of **9b**, **9a@G**, or **9b@G** showed their distinctive molecular ion peaks.

The complexations of free host **9b** were tried by heating (80–170 °C) **9b** in methyl ethyl ketone, DMF, DMA, pyrazine, 1,4-dioxane, *N,N*-dimethylpropionamide, and NMP, but no complexation was observed. This might be due to the larger energy barrier of entrance into the cavity than that actually anticipated by CPK model.¹³

Solution ¹H NMR Spectra of Hemicarceplexes. In case of **9a@DMA** (see Chart 2), its COSY spectrum showed the cross-peaks between CH₂ protons of the R ((CH₂)₂Ph) group and methine protons (H_g) of the A moiety and CH₂ protons of the R' ((CH₂)₂CH₃) group and methine protons (H_h) of the B moiety, respectively. Therefore, the assignments of H_g and H_h protons were determined. Its 2D ROESY spectrum also shows the same cross-peaks (Figure 1). In addition, CH₂ protons of the R and R' groups show the cross-peaks with the aryl protons (H_b) of the A moiety and the aryl protons (H_a) of the B moiety, respectively. This spectrum also shows connectivities between H_i and H_j protons, H_c and H_d protons, and H_e and H_f protons. The assignment of H_c and H_e protons was determined from the cross-peaks between H_e and H_k protons.

The chemical shifts of hydrogens attached to the hemisphere parts of hosts changed upon complexation (Table 1). As expected, the complexed guests generally affect the Δδ values of the H_d and H_f protons more than those of the other protons since these are oriented inward of the cavity. Especially H_f protons, which are inner OCH₂O protons of the B moiety, show the largest downfield shifts ranging from 0.08 to 0.25 ppm upon complexation. The Δδ values for **9b@DMF** range only

(9) (a) Lee, J.; Choi, K.; Paek, K. *Tetrahedron Lett.* **1997**, *38*, 8203. (b) Ihm, C.; Kim, M.; Ihm, H.; Paek, K. *J. Chem. Soc., Perkin Trans. 2* **1999**, 1569.

(10) Sherman, J. C.; Knobler, C. B.; Cram, D. J. *J. Am. Chem. Soc.* **1991**, *113*, 2194.

(11) Cram, D. J.; Jaeger, R.; Deshayes, K. *J. Am. Chem. Soc.* **1993**, *115*, 10111.

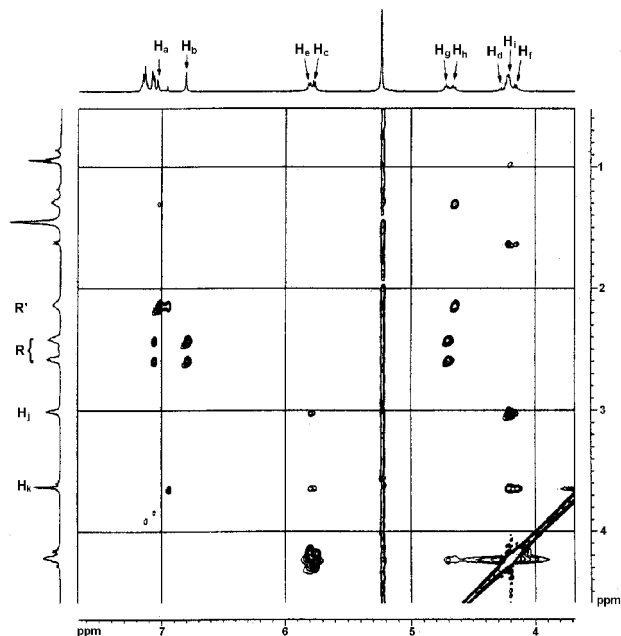
(12) (a) Chapman, R. G.; Chopra, N.; Cochien, E. D.; Sherman, J. C. *J. Am. Chem. Soc.* **1994**, *116*, 369. (b) Nakamura, K.; Sheu, C.; Keating, A. E.; Houk, K. N. *J. Am. Chem. Soc.* **1997**, *119*, 4321. (c) Chapman, R. G.; Sherman, J. *J. Org. Chem.* **1998**, *63*, 4103.

(13) Houk, K. N.; Nakamura, K.; Sheu, C.; Keating, A. E. *Science* **1996**, *273*, 627.

Table 1. Chemical Shifts (in ppm) of Host **9b's Guest-Sensitive Protons and the Differences between the Chemical Shifts of Free and Complexed Hosts ($\Delta\delta$, in Parenthesis)^a in Their 400 MHz ¹H NMR Spectra in CDCl₃ at 25 °C**

guest	chemical shifts								
	H _a	H _b	H _c	H _d	H _e	H _f	H _g	H _h	
none	7.00	6.75	5.89	4.20	5.93	3.97	4.69	4.74	
DMF	7.05	6.76	5.79	4.19	5.89	4.14	4.66	4.76	
	(-0.05)	(-0.01)	(0.10)	(0.01)	(0.04)	(-0.08)	(0.03)	(-0.02)	
DMA	7.05	6.77	5.82	4.30	5.87	4.22	4.68	4.75	
	(-0.05)	(-0.02)	(0.07)	(-0.10)	(0.06)	(-0.25)	(0.01)	(-0.01)	
DMSO	7.03	6.75	5.82	4.24	5.87	4.21	4.69	4.76	
	(-0.03)	(0.00)	(0.07)	(-0.04)	(0.06)	(-0.24)	(0.00)	(-0.02)	
NMP	7.06	6.77	5.85	4.30 ^b	5.87	4.15 ^b	4.67	4.75	
	(-0.06)	(-0.02)	(0.04)	~4.40	(0.06)	~4.25	(0.02)	(-0.01)	

^a $\Delta\delta = \delta_{\text{free}} - \delta_{\text{complexed}}$. ^b Peak is overlapped with H_i proton peak.

**Figure 1.** Part of the 2D ROESY spectrum (500 MHz) of **9a@DMA** at 25 °C in CD₂Cl₂.

from 0.01 to 0.10 ppm. It is likely that complexed DMF is more conformationally mobile in its cavity than complexed DMA, DMSO, and NMP due to its relatively small size. The chemical shift change of H_i cannot be identified due to its multiplicity as well as overlapping. Also, chemical shifts of feet hydrogens (2-phenylethyl or pentyl) do not change upon complexation.

The guest signals were much more sensitive than the host signals to incarceration. Table 2 records the chemical shifts in the 400 MHz ¹H NMR spectra of complexed and free guests as well as their differences ($\Delta\delta$) in host **9a** and **9b** in CDCl₃ at 25 °C.

Upon complexation, the ¹H NMR spectra show large upfield shifts of the guests ranging from 1.19 to 3.50 ppm due to the shielding effect of the two hemispheres of host. As the size of guests increases, the chemical shifts of complexed guests become more upfield shifted because the larger guest approaches more closely to the shielding zone of hemispheres. The similar chemical shifts of DMF or DMA in **9a** and **9b** within the experimental error manifests the magnetic independence between guest and feet (R). H_a of NMP in **9b** showed the largest upfield shift (3.50 ppm), but H_c and H_d of NMP in **9b** showed rather small chemical shift changes (2.89, 2.93 ppm, respectively), which implies that due to the steric effect H_c and H_d cannot get in close to hemisphere's shielding zone.

Table 2. ¹H NMR Spectral Chemical Shifts of Free and Complexed Guests in Hosts **9a and **9b** in Their 400 MHz ¹H NMR Spectra in CDCl₃ at 25 °C**

host	guest	H	free δ	compl δ	$\Delta\delta$
9a	DMF	a	7.99	6.24	1.75
		b	2.94	1.53	1.41
		c	2.86	-0.08	2.94
9a	DMA	a	2.09	-1.33	3.42
		b	3.02	-0.31	3.33
		c	2.94	1.69	1.25
9b	DMF	a	7.99	6.23	1.76
		b	2.94	1.75	1.19
		c	2.86	-0.08	2.94
9b	DMA	a	2.09	-1.34	3.43
		b	3.02	-0.32	3.34
		c	2.94	1.65	1.29
9b	DMSO	a	2.61	-0.34	2.95
		b	2.85	-0.65	3.50
9b	NMP ^a	a	3.40	1.85	1.55
		b	2.05	-0.84	2.89
		c	2.35	-0.58	2.93

^a Major conformer.

Table 3. Half-Lives and Activation Free Energies for Decomplexation of **9b@DMF and **9b@DMA** in C₆D₅NO₂**

complex	$t_{1/2}$ (h)						ΔG^\ddagger (kJ mol ⁻¹)
	150 °C	160 °C	170 °C	180 °C	200 °C	220 °C	
9b@DMF	116.0	57.8	28.9	16.5			104 ± 4
9b@DMA			231.0	116.0	57.8	28.9	73 ± 9

Contrary to this, H_a and H_b of DMA in **9b** showed the similar chemical shift changes (3.43, 3.34 ppm, respectively) owing to their similar steric circumstances.

Decomplexation Kinetics of the Hemispherplexes. The first-order rate constants for decomplexation of hemispherplexes **9b@DMF** and **9b@DMA** were determined in C₆D₅NO₂ at various temperatures in the range of 150–220 °C by watching the decreasing signals of the complexed guest protons and/or the appearance of the free guest proton's signals.⁵ Interestingly, complexed DMA gave doublets (or two singlets) for each hydrogen, which is totally unexpected because DMA can freely rotate through the long C₄ axis as well as the short equatorial axis at least at 220 °C.

The decomplexations exhibited good first-order behavior. Table 3 records the half-lives for decomplexations at various temperatures and the derived free energies of activation for decomplexation. The decomplexation half-

life for **9b@DMA** is about seven times longer than that for **9b@DMF** at the same temperature. This is possibly due to the fact that the longer DMA guest should pass from occupying the host's axial bowls to being aligned with the equatorially disposed portals. But free energy of activation for decomplexation of **9b@DMF** is 31 kJ mol⁻¹ higher than that for **9b@DMA**. Presumably, the steric compression in **9b@DMA** is greater than that in **9b@DMF**, and therefore, **9b@DMA** reaches more easily to transition states for decomplexation.

Energy Barriers for Free Rotation around the C(=O)–N Amide Bonds of Complexed DMA and DMF. The rotational barrier to amide bonds has been extensively studied in solution and in the gas phase, experimentally and theoretically.¹⁴ The energy barriers decrease in the order of polar solvents > nonpolar solvents > gas phase. Generally, the energy barrier for DMF is larger than for DMA. This difference is mainly caused by destabilization of the ground state in DMA due to steric repulsion rather than by a difference in the energy of the transition state.

Dynamic ¹H NMR experiments were performed to compare the energy barrier for free rotation around the amide bond of complexed and free amide guests in DMSO-*d*₆ or C₆D₅NO₂ as a solvent. The coalescence temperature for two NCH₃ groups of **9a@DMA** in C₆D₅NO₂ was 151 °C with $\Delta G_{424K}^\ddagger = 18.6$ kcal mol⁻¹ for complexed amide rotation around its C(=O)–N bond. In DMSO-*d*₆, the same coalescence temperature was observed. For DMA simply dissolved in C₆D₅NO₂, the reported coalescence temperature was 63 °C and $\Delta G_{336K}^\ddagger = 18.0$ kcal mol⁻¹.¹⁰

When **9b@DMF** was submitted to the same experiment in C₆D₅NO₂, the coalescence temperature was assumed to be over 161 °C. The coalescence of DMF dissolved directly in C₆D₅NO₂ was reported to be 120 °C with $\Delta G_{393K}^\ddagger = 20.2$ kcal mol⁻¹.¹⁰ In agreement with known results, the barrier of complexed DMF was observed to be higher than that for complexed DMA.

Incarceration of DMA or DMF raises the rotational barrier compared to its simple dissolution. This behavior is probably a result of steric constriction on guest by incarceration. Also the energy barrier of complexed DMA was not affected by the polarity change of solvent within experimental error because DMA is enclosed by the shell of the host.

Orientations of Guests Inside Hemicarcerands: Carceroisomerism. Interestingly, the acetyl peaks (MeC=O) of DMA and the aldehydic peaks (HC=O) of DMF did not change their doublet pattern in ¹H NMR spectra even though the temperature was increased to 187 °C. Essentially, the peaks should coalesce into singlets on the increase of the temperature allowing rapid isomerization if each of doublet were caused by the different orientation (carceroisomers) of the guests in the shell.^{7a}

The dynamic behavior of complexed guest was studied by variable-temperature ¹H NMR experiments, and the orientations of the guests of major isomers were determined by 2D NOESY and ROESY measurements.

As shown in Figure 2a, at a temperature below –90 °C, ¹H NMR spectra of **9a@DMA** show two new resonances at $\delta = -0.24$ (doublet, minor) and –0.72 (singlet,

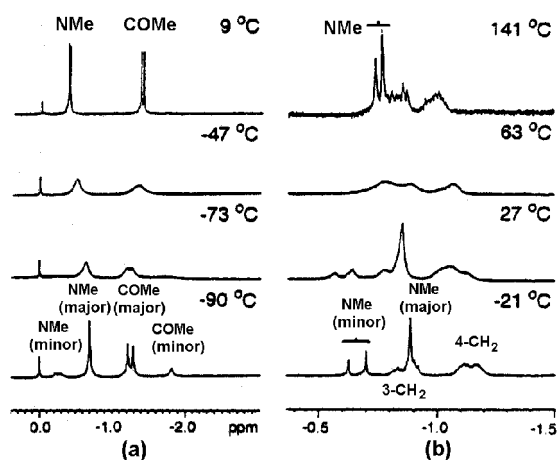


Figure 2. Partial ¹H NMR spectra (500 MHz) of (a) **9a@DMA** and (b) **9b@NMP** (in C₆D₅NO₂ at 63 and 141 °C) in CD₂Cl₂ at various temperatures.

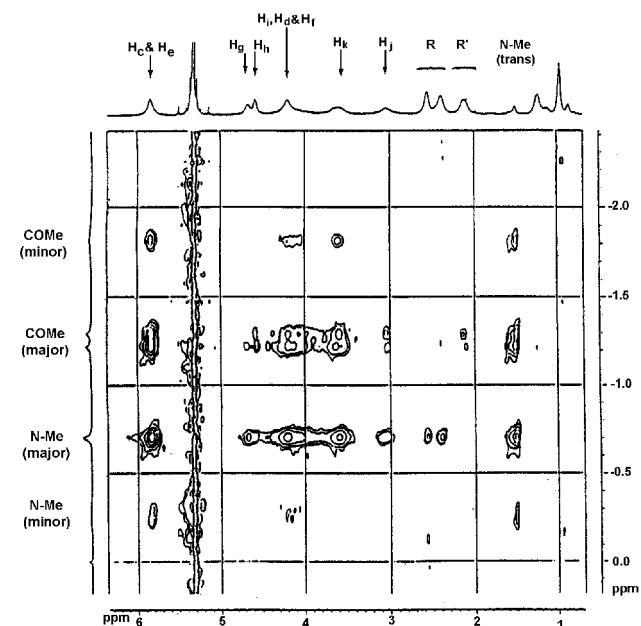


Figure 3. Part of the 2D NOESY spectrum (500 MHz) at –90 °C in CD₂Cl₂ of **9a@DMA**.

major) for the *N*-methyl group cis to the carbonyl of DMA and at $\delta = -1.26$ (doublet, major) and –1.83 (singlet, minor) for the acetyl group of DMA, respectively. The integration ratio of major to minor signal is 3:1.

2D NOESY spectrum (Figure 3) of **9a@DMA** showed that the major doublet signal at $\delta = -1.26$ corresponds to the isomer in which the acetyl group is positioned close to the **B** moiety (Chart 2) from its cross-peaks with the resonances of the aryl protons (H_a), the methine CH protons (H_b) and the R' groups (propyl groups) of the **B** moiety, whereas the major singlet signal at $\delta = -0.72$ showed cross-peaks with the resonances of the aryl protons (H_b), the methine CH protons (H_g), and the R groups (2-phenylethyl group) of the **A** moiety, which means the *N*-methyl group cis to the carbonyl is oriented toward the **A** moiety. Accordingly, the minor signals at $\delta = -0.83$ and –0.24 are from the opposite orientation of DMA relative to the major conformer, which gave too weak NOEs. These results support that two carceroisomers exist in a 3:1 ratio and the acetyl group of DMA is mainly oriented toward the **B** moiety as shown in

(14) Wiberg, K. B.; Rablen, P. R.; Rush, D. J.; Keith, T. A. *J. Am. Chem. Soc.* **1995**, *117*, 4261.

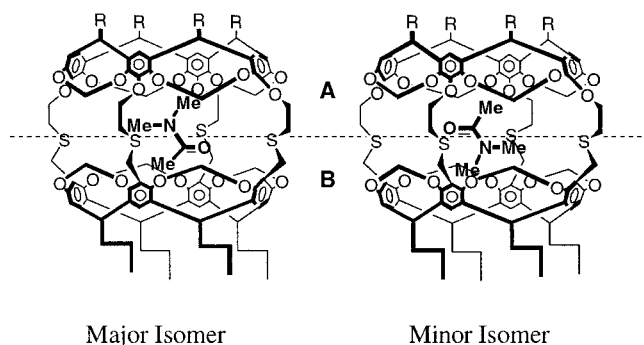


Figure 4. Observed orientation of DMA in the major isomer (left) and in the minor isomer (right) of **9a@DMA** ($R = (\text{CH}_2)_2\text{Ph}$).

Figure 4 below -90°C in CD_2Cl_2 . **9b@DMA** gave the same results showing that the behavior of the guest inside the host is not affected by feet of the host.

When the temperature of **9b@DMF** is lowered to -81°C its ^1H NMR spectra show that each guest's signal changes into doublets for the CHO proton at $\delta = 6.21$ and for the *N*-methyl group trans to the carbonyl at $\delta = -0.31$ and -1.04 at 1:1 integration ratios. NOESY experiments at a temperature below -81°C revealed both doublets of the *N*-methyl protons show cross-peaks with the resonances of the **B** moiety. Therefore, it is assumed that two doublet signals of DMF were caused by an unusual circumstance of the host **B** moiety and not by carceroisomerism of DMF even though the structural elucidation of two isomers was not confirmed due to weak NOE connectivities.

When **9b@DMSO** was subjected to the similar ^1H NMR experiment, their end-to-end rotation inside the host was too fast to observe two carceroisomers in ^1H NMR time scale even at a temperature below -116°C .

Interestingly, VT NMR experiment of **9b@NMP** showed the presence of unequal populations of two carceroisomers even at 141°C (Figure 2b). At a temperature below -21°C , the spectrum of **9b@NMP** showed clearly that the *N*-methyl group of incarcerated NMP exists in major (the singlet at $\delta = -0.89$) and minor (two unequal singlets at $\delta = -0.63$ and -0.70) isomers. The multiplets (actually two kinds of multiplet) at $\delta = -0.86$ and -1.12 is assigned to the 3- CH_2 and 4- CH_2 groups, respectively. The 5- CH_2 group of NMP resonates at much lower field of $\delta = 1.85$, since it is far away from the aromatic cavity. The integration ratio of major to minor signal is 2:1.

2D NOESY experiments of **9b@NMP** at -21°C revealed that the 4- CH_2 group of NMP shows strong cross-peaks with H_i and H_k , which means these protons are mainly oriented toward the **B** moiety although it is difficult to discriminate between the major and minor isomer (Figure 5). The major singlet signal of the *N*-methyl group at $\delta = -0.89$ and the 3- CH_2 group of NMP at -0.86 show cross-peaks with the resonances of the protons of the bridging unit near the **A** moiety (H_i) and of the inner OCH_2O protons (H_j) of the **B** moiety, but these protons cannot be discriminated due to overlapped peaks, whereas the minor doublet signal of the *N*-methyl group at $\delta = -0.66$ shows a cross-peak with H_j , which means that this methyl group in the minor isomer is located in the **B** moiety. This suggests that *N*-methyl group is mainly oriented toward the **A** moiety in the major isomer (Figure 5).

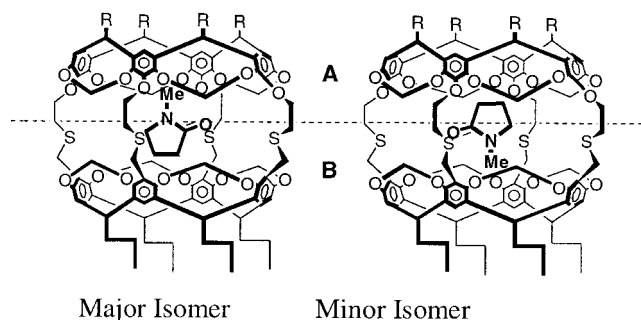


Figure 5. Observed orientation of NMP in the major (left) and minor isomer (right) of **9b@NMP** ($R = (\text{CH}_2)_4\text{CH}_3$).

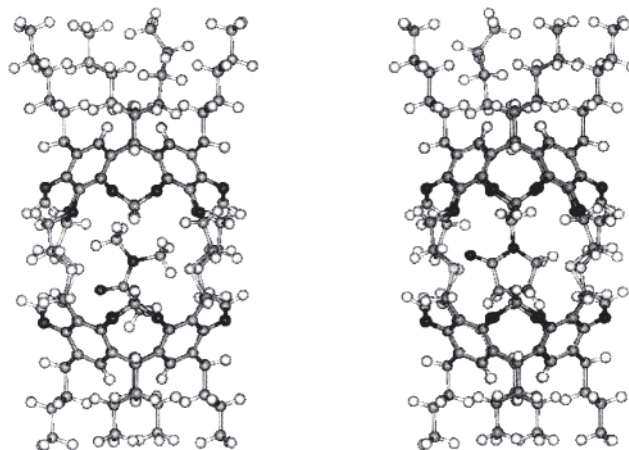


Figure 6. Energy-minimized structures of hemicarceplexes **9b@DMA** (left) and **9b@NMP** (right).

Identification of Half-Twistomers. Figure 6 shows the energy-minimized structures of **9b@DMA** and **9b@NMP** calculated with MM+ force-field using HyperChem. The results correspond closely to the structure of the major isomers observed in their ^1H NMR spectra.

As shown in Figure 2a, ^1H NMR chemical shifts of DMA in host **9a** appeared as two equal singlets at room temperature, which remained up to 187°C . As the temperature of **9a@DMA** in CD_2Cl_2 decreased, two singlets were broadened, and then below -90°C , the chemical shifts of incarcerated DMA were split into two new resonances indicating the existence of carceroisomers. But the interesting point is the presence of two singlets at -0.24 and -1.26 ppm for the thiahemisphere-directing trans *N*-methyl of minor carceroisomer and for the thiahemisphere-directing acetyl group of major carceroisomers, respectively, which, we assumed, is due to the stable twistomerism at thiahemisphere moiety (**B**). These half-twistomers did not coalesce each other, but two carceroisomers coalesced each other by the rapid end-to-end rotation of DMA vertical to C_4 axis to give two sets of two singlets at -0.31 ppm for trans *N*-methyl and at -1.33 ppm for acetyl at high temperature.

The simultaneous observation of twistomers and carceroisomers of **9b@NMP** under the same conditions was possible even at 25°C (Figure 2b). At a temperature below -21°C , the ^1H NMR chemical shifts of *N*-methyl group of **9b@NMP** clearly showed that carceplex **9b@NMP** exists in the major (the singlet at $\delta = -0.89$) and minor (two unequal singlets at $\delta = -0.63$ and -0.70) carceroisomers at 2:1. The two unequal singlets of minor isomer implies that the stabilities of two twistomers are

Table 4. Rate Constant (*k*), Coalescence Temperature (*T_c*), and Rotational Barrier (ΔG_c^\ddagger) for Isomerization of Two Carceroisomers^a

host	guest	<i>k</i> (Hz)	<i>T_c</i> (°C)	ΔG_c^\ddagger (kcal mol ⁻¹)
9a	DMA	5592	-61	9.6 ± 1
9b	DMA	6002	-61	9.6 ± 1
9b	DMF	773	-39	10.5 ± 1
9b	DMSO		<-116	
9b	NMP	255	50	15.4 ± 1

^a Determined by variable-temperature ¹H NMR (500 MHz, CD₂Cl₂) experiments.

different each other due to the prochirality of NMP. Its NOESY experiments in CD₂Cl₂ at -21 °C showed that *N*-methyl group of the major isomer is directing the **A** moiety (Figure 5).

A CPK molecular model shows that the cavity of the **B** moiety is smaller than that of the **A** moiety due to the inward-directing sulfur atoms. ¹H NMR spectra in Figure 4 show that the guest's peaks located in the **B** moiety are split into the doublet, slightly downfield shifted, whereas the peaks located in the **A** moiety are not split and more upfield shifted. It is probable that the twistomer isomerization at **A** moiety is faster on an ¹H NMR time scale but that at the **B** moiety is slower on an ¹H NMR time scale due to the large rotational barrier of thia bonds, which results in the unprecedented half-twistomerism.

Isomerization Energy Barriers for Carceroisomers. Table 4 records the isomerization energy barriers of carceroisomers determined by variable-temperature NMR experiments. In the case of **9a@DMA**, the two carceroisomers coalesced at -61 °C and the rotational barrier (ΔG_{212K}^\ddagger) for isomerization was calculated to be 9.6 ± 1 kcal mol⁻¹. For **9a** and **9b**, having different feet, the activation energies for interconversion of complexed DMA are consistent with each other.

The ΔG_c^\ddagger of **9b@DMF** is rather higher than that of **9b@DMA**. It means DMF inside the host exists in two types of substantially stable isomers. If not, the coalescence temperature of DMF should be lower than for DMA due to its smaller size.

The coalescence temperature of **9b@DMSO** is below -116 °C, which suggests that end-to-end rotation of the DMSO molecule inside the host is fast in ¹H NMR time scale even at a temperature below -116 °C.

Upon warming to 50 °C, the *N*-methyl proton peaks of NMP were coalesced to give $\Delta G_c^\ddagger = 15.4 \pm 1$ kcal mol⁻¹ for the rotational barrier of interconversion of NMP inside the cavity, which is 5.8 kcal mol⁻¹ higher than that for **9b@DMA** primarily due to its larger size and rigidity.

When the temperature of **9b@NMP** was increased until 141 °C in C₆D₅NO₂, the *N*-methyl proton peak of NMP still remained as two singlets, which is similar to those of **9b@DMA** and **9b@DMF**.

Conclusions

Resorcin[4]arene-based tetraoxatetrathiahemicarceplexes were synthesized by shell closure of a tetrathio-cavitand and a tetraiodocavitand, which possess a non-centrosymmetric *C*_{4v} cavity, and therefore, different orientations of incarcerated unsymmetric guest could give different stereoisomers.

The first-order rate for decomplexation of hemicarceplexes was determined by ¹H NMR experiments, and the free energy of activation for decomplexation of

9b@DMF is 31 kJ mol⁻¹ higher than that for **9b@DMA**. The dynamic NMR experiments of hemicarceplexes revealed that the energy barriers for rotation around the amide bonds of complexed DMA and DMF are higher than those of free DMA and DMF.

Orientations of the guests inside the hosts were studied by 2D NOESY and ROESY NMR experiments. Two carcerostereoisomers of **9a@DMA** or **9b@DMA** appeared as 3:1 ratio at -90 °C in CD₂Cl₂, and they coalesced at -61 °C, which gave the isomerization barrier of $\Delta G^\ddagger = 9.6 \pm 1$ kcal mol⁻¹. **9b@NMP** showed two carcerostereoisomers (2:1 ratio) at -21 °C in CD₂Cl₂ that are coalesced at 50 °C to show the higher isomerization barrier ($\Delta G^\ddagger = 15.4 \pm 1$ kcal mol⁻¹). The acetyl group of DMA or 3- and 4-CH₂ units of NMP in **9b** are mainly directed toward the **B** moiety surrounded by sulfur atoms at low temperatures at which the acetyl group of major **9b@DMA** or NCH₃ of minor **9b@NMP** gave doublets on ¹H NMR spectra due to their half-twistomerism. These doublets were coalesced with their counterparts to give new doublets at high temperature, which means these half-twistomers induced by incorporating unsymmetrical thia bridges between two hemispheres are unexpectedly stable even at substantially high temperature.

Such high isomerization energy barriers for supramolecular carceroisomers or twistomers may present an opportunity for the development of unprecedented molecular devices. For example, if methods could be found to control the supramolecular isomerization, then such materials could be used to re-align guests by acting as switchable matrixes.

Experimental Section

General Procedures. All chemicals were reagent grades and used directly unless otherwise specified. THF was stored over calcium hydride for 1 week and was freshly distilled under N₂ from sodium benzophenone ketyl just prior to use. All anhydrous reactions were conducted under an argon atmosphere. Melting points were measured on an Electrothermal 9100 apparatus and were uncorrected. IR spectra were taken with a Mattson 3000 FT-IR spectrometer. The ¹H NMR spectra were recorded on a Bruker Avance DPX300 (300 MHz), JEOL lambda-400 (400 MHz), or Bruker Avance DPX500 (500 MHz) in CDCl₃ unless stated otherwise, and residual solvent protons were used as internal standard. FAB(+) mass spectra were run on a HR MS (VG70-VSEQ) at Korea Basic Science Institute using *m*-nitrobenzyl alcohol as a matrix. Gravity column chromatography was performed on silica gel 60 (E. Merck, 70-230 mesh ASTM). Flash chromatography was performed on silica gel 60 (E. Merck, 230-400 mesh ASTM). Thin-layer chromatography was done on silica plastic sheets (E. Merck, silica gel 60 F254, 0.2 mm). Elemental analyses were performed at the Korea Basic Science Institute.

2,20:3,19-Dimetheno-1H,21H,23H,25H-bis[1,3]dioxocino[5,4-*f*5',4'-*f'*]benzo[1,2-*d*5,4-*d'*]bis[1,3]benzodioxocin, 7,11,15,28-Tetrakis(2-chloroethoxy)-1,21,23,25-terakis(2-phenylethyl)-, Stereoisomer (5). To a solution of tetrol **3** (0.51 g, 0.50 mmol) and potassium carbonate (0.69 g, 5.0 mmol) in DMF (30 mL) was added 2-chloroethane tosylate (0.71 g, 3.0 mmol), and the reaction mixture was stirred for 3 d at 55-60 °C. After being cooled to room temperature, the mixture was partitioned between CH₂Cl₂ (250 mL) and 2 N HCl (2 × 100 mL). The organic phase was separated, washed with water and brine, and subsequently dried over MgSO₄. After evaporation of CH₂Cl₂, the residue was chromatographed on a silica gel gravity column using CH₂Cl₂-hexane (3:1, v/v) and then hexanes-EtOAc (3:1, v/v). The recrystallization from CH₂Cl₂-MeOH gave the product **5** (0.43 g, 69%): mp 269.7 °C; ¹H NMR (CDCl₃, 400 MHz) δ 7.21-7.13 (m, ArH, 20H), 6.85 (s, ArH,

4H), 5.85 (d, OCH₂O, *J* = 7.1 Hz, 4H), 4.83 (t, ArCH, 4H), 4.43 (d, OCH₂O, *J* = 7.1 Hz, 4H), 4.18 (t, OCH₂, 8H), 3.71 (t, CH₂Cl, 8H), 2.68 (m, PhCH₂, 8H), 2.48 (m, PhCH₂CH₂, 8H).

2,20:3,19-Dimetheno-1*H*,21*H*,23*H*,25*H*-bis[1,3]dioxocino[5,4-*i*:5',4'-*f'*]benzo[1,2-*d*:5,4-*d'*]bis[1,3]benzodioxocin, 7,11,15,28-Tetrakis(2-chloroethoxy)-1,21,23,25-terapentyl-, Stereoisomer (6). The procedure for compound **5** was followed with tetrol **4** (0.50 g, 0.57 mmol), potassium carbonate (0.79 g, 5.7 mmol) in DMF (30 mL) and 2-chloroethane tosylate (1.1 g, 4.5 mmol) to obtain product **6** (0.42 g, 65%): mp 255.6–257.6 °C; ¹H NMR (CDCl₃, 300 MHz) δ 6.80 (s, ArH, 4H), 5.82 (d, OCH₂O, *J* = 7.2 Hz, 4H), 4.70 (t, ArCH, 4H), 4.39 (d, OCH₂O, *J* = 7.2 Hz, 4H), 4.16 (t, OCH₂, 8H), 3.69 (t, CH₂Cl, 8H), 2.17 (m, CH₂, 8H), 1.40–1.23 (m, CH₂, 24H), 0.92 (t, CH₃, 12H).

2,20:3,19-Dimetheno-1*H*,21*H*,23*H*,25*H*-bis[1,3]dioxocino[5,4-*i*:5',4'-*f'*]benzo[1,2-*d*:5,4-*d'*]bis[1,3]benzodioxocin, 7,11,15,28-Tetrakis(2-iodoethoxy)-1,21,23,25-terakis(2-phenylethyl)-, Stereoisomer (7). A solution of sodium iodide (118 mg, 0.79 mmol) in MEK (30 mL) was refluxed for 1 h. To a refluxing solution was added tetrachloride **5** (100 mg, 0.079 mmol) and the mixture refluxed for 3 d. After evaporation of MEK, the crude mixture was taken up in CH₂-Cl₂ (100 mL), washed with water (2 × 100 mL) and brine (25 mL), and subsequently dried over MgSO₄. After evaporation of CH₂Cl₂, the crude product was recrystallized from CH₂Cl₂-MeOH to give the product **7** (112 mg, 87%) as a white powder: mp 279.5 °C; ¹H NMR (CDCl₃, 400 MHz) δ 7.28–7.16 (m, ArH, 20H), 6.86 (s, ArH, 4H), 5.92 (d, OCH₂O, *J* = 7.1 Hz, 4H), 4.83 (t, ArCH, 4H), 4.44 (d, OCH₂O, *J* = 7.1 Hz, 4H), 4.19 (t, OCH₂, 8H), 3.37 (t, CH₂I, 8H), 2.70 (m, PhCH₂, 8H), 2.49 (m, PhCH₂CH₂, 8H).

2,20:3,19-Dimetheno-1*H*,21*H*,23*H*,25*H*-bis[1,3]dioxocino[5,4-*i*:5',4'-*f'*]benzo[1,2-*d*:5,4-*d'*]bis[1,3]benzodioxocin, 7,11,15,28-Tetrakis(2-iodoethoxy)-1,21,23,25-terapentyl-, Stereoisomer (8). The procedure for compound **7** was followed with sodium iodide (0.79 g, 5.3 mmol) in MEK (40 mL) and tetrachloride **6** (0.18 g, 0.53 mmol) to obtain product **8** (0.76 g, 90%) as a white powder: mp 213.1–216.4 °C; ¹H NMR (CDCl₃, 300 MHz) δ 6.82 (s, ArH, 4H), 5.87 (d, OCH₂O, *J* = 7.2 Hz, 4H), 4.69 (t, ArCH, 4H), 4.39 (d, OCH₂O, *J* = 7.2 Hz, 4H), 4.15 (t, OCH₂, 8H), 3.34 (t, CH₂I, 8H), 2.17 (m, CH₂, 8H), 1.40–1.14 (m, CH₂, 24H), 0.93 (t, CH₃, 12H).

General Procedure of Hemicarceplexes (9@G). Under argon atmosphere, a solution of tetraiodide **7** or **8** (0.25 g, 0.17 mmol) and tetrathiol **2** (0.18 g, 0.20 mmol) in solvent G (60 mL) was added dropwise to a suspension of Cs₂CO₃ (0.55 g, 1.7 mmol) in solvent G (100 mL) for 8 h at 50 °C. The mixture was stirred for another 12 h, and then the temperature was increased into 80 °C followed by stirring for 3 h. After being cooled to room temperature, the solvent was taken up in CH₂Cl₂ (300 mL), washed with 2 N HCl (80 mL), H₂O (3 × 200 mL), and brine (50 mL), and dried over MgSO₄. After evaporation of the solvent, the crude mixture was purified by flash column chromatography (SiO₂, EtOAc/hexane = 1/9).

Hemicarceplex (9a@DMF): yield 8%; mp > 266 °C dec; FT-IR (KBr) 1682 cm⁻¹ (ν_{C=O}); ¹H NMR (CDCl₃, 400 MHz) δ 7.08 (s, ArH_a, 4H), 6.82 (s, ArH_b, 4H), 6.24 (d, COH, 1H), 5.86 (d, OCH₂eO, *J* = 7.1 Hz, 4H), 5.77 (d, OCH₂cO, *J* = 7.1 Hz, 4H), 4.74 (t, ArCH_g, 4H), 4.73 (t, ArCH_h, 4H), 4.22 (s, OCH₂i, 8H), 4.14 (d, OCH₂dO, *J* = 7.1 Hz, 4H), 4.11 (d, OCH₂fO, *J* = 7.1 Hz, 4H), 3.64 (s, ArCH₂kS, 8H), 3.03 (s, SCH₂j, 8H), 2.60 (m, PhCH₂, 8H), 2.40 (m, PhCH₂CH₂, 8H), 2.10 (m, CH₂, 8H), 1.53 (d, NCH₃, 3H), 1.19 (m, CH₂, 8H), 0.95 (t, CH₃, 12H), -0.08 (d, NCH₃, 3H).

Hemicarceplex (9a@DMA): yield 11%; mp > 274 °C dec; FT-IR (KBr) 1658 cm⁻¹ (ν_{C=O}); ¹H NMR (CDCl₃, 400 MHz) δ 7.13 (s, ArH_a, 4H), 6.82 (s, ArH_b, 4H), 5.89 (d, OCH₂eO, *J* = 7.1 Hz, 4H), 5.85 (d, OCH₂cO, *J* = 7.1 Hz, 4H), 4.81 (t, ArCH_g, 4H), 4.76 (t, ArCH_h, 4H), 4.34 (d, OCH₂dO, *J* = 7.1 Hz, 4H), 4.30 (s, OCH₂i, 8H), 4.23 (d, OCH₂fO, *J* = 7.1 Hz, 4H), 3.70 (s, ArCH₂kS, 8H), 3.08 (s, SCH₂j, 8H), 2.65 (m, PhCH₂, 8H), 2.44 (m, PhCH₂CH₂, 8H), 2.16 (m, CH₂, 8H), 1.69 (d, NCH₃, 3H), 1.23 (m, CH₂, 8H), 0.99 (t, CH₃, 12H), -0.31 (d, NCH₃, 3H), -1.33 (d, COCH₃, 3H). Anal. Calcd for C₁₂₀H₁₂₉O₂₁N₁S₄

CH₃OH·4H₂O: C, 68.19; H, 6.46; N, 0.64. Found: C, 68.18; H, 6.32; N, 0.64.

Hemicarceplex (9b@DMF): yield 13%; mp > 267 °C dec; FT-IR (KBr) 1682 cm⁻¹ (ν_{C=O}); ¹H NMR (CDCl₃, 400 MHz) δ 7.05 (s, ArH_a, 4H), 6.76 (s, ArH_b, 4H), 6.23 (d, COH, 1H), 5.89 (d, OCH₂eO, *J* = 7.3 Hz, 4H), 5.79 (d, OCH₂cO, *J* = 7.3 Hz, 4H), 4.76 (t, ArCH_h, 4H), 4.66 (t, ArCH_g, 4H), 4.25 (s, OCH₂i, 8H), 4.19 (d, OCH₂dO, *J* = 7.3 Hz, 4H), 4.14 (d, OCH₂fO, *J* = 7.3 Hz, 4H), 3.67 (s, ArCH₂kS, 8H), 3.06 (s, SCH₂j, 8H), 2.16 (m, CH₂, 16H), 1.75 (d, NCH₃, 3H), 1.37–1.23 (m, CH₂, 32H), 0.99–0.89 (m, CH₃, 24H), -0.08 (d, NCH₃, 3H); FAB(+) MS *m/z* 1948 (9b@DMF⁺, 100), 1875 (9b⁺, 8). Anal. Calcd for C₁₁₁H₁₃₅O₂₁N₁S₄·5H₂O: C, 65.43; H, 7.17. Found: C, 65.56; H, 6.93.

Hemicarceplex (9b@DMA): yield 25%; mp > 259 °C dec; FT-IR (KBr) 1658 cm⁻¹ (ν_{C=O}); ¹H NMR (CDCl₃, 400 MHz) δ 7.05 (s, ArH_a, 4H), 6.77 (s, ArH_b, 4H), 5.87 (d, OCH₂eO, *J* = 7.3 Hz, 4H), 5.82 (d, OCH₂cO, *J* = 7.3 Hz, 4H), 4.75 (t, ArCH_h, 4H), 4.68 (t, ArCH_g, 4H), 4.30 (d, OCH₂dO, *J* = 7.3 Hz, 4H), 4.27 (s, OCH₂i, 8H), 4.22 (d, OCH₂fO, *J* = 7.3 Hz, 4H), 3.69 (s, ArCH₂kS, 8H), 3.06 (s, SCH₂j, 8H), 2.17 (m, CH₂, 16H), 1.65 (d, NCH₃, 3H), 1.37–1.23 (m, CH₂, 32H), 1.00–0.84 (m, CH₃, 24H), -0.32 (d, NCH₃, 3H), -1.34 (d, COCH₃, 3H); FAB(+) MS *m/z* 1962 (9b@DMA⁺, 82), 1874 (9b⁺, 23). Anal. Calcd for C₁₁₂H₁₃₇O₂₁N₁S₄·CH₃OH·3H₂O: C, 66.28; H, 7.24; N, 0.68. Found: C, 66.25; H, 7.16; N, 0.52.

Hemicarceplex (9b@DMSO): yield 10%; mp > 248 °C dec; ¹H NMR (CDCl₃, 400 MHz) δ 7.03 (s, ArH_a, 4H), 6.75 (s, ArH_b, 4H), 5.87 (d, OCH₂eO, *J* = 7.3 Hz, 4H), 5.82 (d, OCH₂cO, *J* = 7.3 Hz, 4H), 4.76 (t, ArCH_h, 4H), 4.69 (t, ArCH_g, 4H), 4.27 (s, OCH₂i, 8H), 4.24 (d, OCH₂dO, *J* = 7.3 Hz, 4H), 4.21 (d, OCH₂fO, *J* = 7.3 Hz, 4H), 3.70 (s, ArCH₂kS, 8H), 3.06 (s, SCH₂j, 8H), 2.15 (m, CH₂, 16H), 1.37–1.23 (m, CH₂, 32H), 1.01–0.88 (m, CH₃, 24H), -0.34 (d, SCH₃, 6H); FAB(+) MS *m/z* 1953 (9b@DMSO⁺, 100). Anal. Calcd for C₁₁₀H₁₃₄O₂₁S₅: C, 67.67; H, 6.92. Found: C, 67.43; H, 7.09.

Hemicarceplex (9b@NMP): yield 13%; mp > 263 °C dec; ¹H NMR (CDCl₃, 400 MHz) δ 7.06 (s, ArH_a, 4H), 6.77 (s, ArH_b, 4H), 5.87 (d, OCH₂eO, 4H), 5.85 (d, OCH₂cO, 4H), 4.75 (t, ArCH_h, 4H), 4.67 (t, ArCH_g, 4H), 4.26–4.09 (m, OCH₂i, OCH₂d,fO, 16H), 3.71 (s, ArCH₂kS, 8H), 3.06 (s, SCH₂j, 8H), 2.15 (m, CH₂, 16H), 1.85 (m, NCH₃, 2H), 1.35–1.23 (m, CH₂, 32H), 1.01–0.86 (m, CH₃, 24H), -0.58 (m, COCH₂, 2H), -0.65 (s, NCH₃, 3H), -0.84 (m, NCH₂CH₂, 2H); FAB(+) MS, *m/z* 1974 (9b@NMP⁺, 100), 1874 (9b⁺, 18). Anal. Calcd for C₁₁₃H₁₃₇O₂₁N₁S₄·CH₂Cl₂: C, 66.52; H, 6.81. Found: C, 66.30; H, 6.98.

Free Hemicarcerand (9b). Under argon atmosphere, a solution of tetrathiol **2** (0.29 g, 0.32 mmol) in acetonitrile (60 mL) was added dropwise to a refluxing solution of tetraiodide **8** (0.40 g, 0.27 mmol) and Cs₂CO₃ (0.87 g, 2.7 mmol) in acetonitrile (120 mL) for 12 h. The mixture was refluxed for another 1 d. After evaporation of acetonitrile, the crude mixture was taken up in CH₂Cl₂ (300 mL), washed with 2 N HCl (80 mL), H₂O (3 × 200 mL), and brine (50 mL), and dried over MgSO₄. After evaporation of CH₂Cl₂, the residue was chromatographed on a silica gel column using hexanes–EtOAc (9:1, v/v) and the recrystallization from CH₂Cl₂-MeOH gave the product **9b** as a white powder (98 mg, 20%): mp > 258 °C dec; ¹H NMR (CDCl₃, 400 MHz) δ 7.00 (s, ArH_a, 4H), 6.75 (s, ArH_b, 4H), 5.93 (d, OCH₂eO, 4H), 5.89 (d, OCH₂cO, 4H), 4.74 (t, ArCH_h, 4H), 4.69 (t, ArCH_g, 4H), 4.25 (s, OCH₂i, 8H), 4.20 (d, OCH₂dO, 4H), 3.97 (d, OCH₂fO, 4H), 3.61 (s, ArCH₂kS, 8H), 3.07 (s, SCH₂j, 8H), 2.09 (m, CH₂, 16H), 1.34–1.23 (m, CH₂, 32H), 1.00–0.85 (m, CH₃, 24H); FAB(+) MS *m/z* 1874 (M⁺, 5). Anal. Calcd for C₁₀₈H₁₂₈O₂₀S₄·3CH₂Cl₂: C, 62.62; H, 6.34. Found: C, 62.33; H, 6.48.

Kinetics of Decomplexation of 9b@DMF and 9b@DMA. Decomplexation kinetics were conducted on 0.5 mL samples of 2 mM solutions of complexes in degassed C₆D₅NO₂ in sealed ¹H NMR tubes in a temperature-controlled (± 1 °C), insulated oil bath. Each tubes were removed at timed intervals and detected by a 400 MHz ¹H NMR spectrometer. About eight spectra were collected for each temperature. Plots of -ln(A/A₀) vs time gave good straight lines that provided first-order rate constants (*k*) for decomplexation (eq 1). The activation

free energies of decomplexation (ΔG^\ddagger) were obtained from the slope of the linear plot of $\ln k$ vs $1/T$ (eq 2).

$$\ln(A/A_0) = -kt \quad (1)$$

$$\ln k = \ln A - \Delta G^\ddagger/RT \quad (2)$$

NMR Measurements. Structure Determination. All dynamic NMR measurements were performed on a Bruker Avance DPX300 (300 MHz) or Bruker Avance DPX500 (500 MHz) spectrometer. NOESY, ROESY, and COSY measurements were carried out with 5 mm QNP ^1H probehead. All NOESY experiments were performed with mixing times between 250 and 650 ms. The probe temperatures were calibrated against 80% ethylene glycol in DMSO- d_6 (for high temperature) and 4% methanol in methanol- d_4 (for low temperature) as standard.

Determination of Rotational Barriers around the Amide Bond of Incarcerated DMF and DMA. The rotational energy barriers around the amide bonds of **9a@DMA** and **9b@DMF** were determined by measuring dynamic ^1H NMR at different temperatures from 25 to 187 °C in $\text{C}_6\text{D}_5\text{NO}_2$ or DMSO- d_6 . From the coalescence temperature, ΔG_c^\ddagger values (kcal mol^{-1}) were calculated with eq 3¹⁵

(15) Friebolin, H. *Basic One- and Two-Dimensional NMR Spectroscopy*; Wille, E. E., Ed.; VCH verlagsgesellschaft mbH Press: Weinheim, 1991.

$$\Delta G_c^\ddagger = 4.58 T_c [9.972 + \log(T_c/\Delta\nu)] \times 10^{-3} \text{ kcal mol}^{-1} \quad (3)$$

where $\Delta\nu$ is the separation in Hz between the two signals.

Determination of Energy Barriers for Interconversion of Carceroisomers. The energy barriers for interconversion between the different orientations of **9a@DMA**, **9b@DMA**, **9b@DMF**, **9b@DMSO**, and **9b@NMP** were determined by measuring the dynamic ^1H NMR at various temperatures from +27 to -98 °C in CD_2Cl_2 . For **9b@NMP**, additional spectra were taken from 27 to 141 °C in $\text{C}_6\text{D}_5\text{NO}_2$. From the coalescence temperatures ΔG_c^\ddagger values (kcal mol^{-1}) were calculated with eq 3 above. Also, the first-order rate constants (k) were calculated with eq 4. The orientation of incarcerated DMA in the major carceroisomer was determined by NOESY and ROESY measurements at -90 °C. The orientation of NMP in the major carceroisomer was determined at -21 °C.

$$k = \pi\Delta\nu/1.414 \quad (4)$$

Acknowledgment. Financial support from the Korea Science and Engineering Foundation (No. 1999-2-123-001-3) and the Korea Research Foundation (KRF-2000-015-DP0196) is gratefully acknowledged.

JO015594I